

Location dependent flight cost differences from the lunar surface and its influence on ISRU location selection

Sven J. Steinert^{1,*}, Paul Zabel² and Dominik Quantius²

¹*Laboratory X, Institute X, School of Engineering and Design, Technical University of Munich (TUM), Munich, Germany*

²*Laboratory X, Institute of Space Systems, Systemanalyse Raumsegment, German Aerospace Center (DLR), Bremen, Germany*

Correspondence*:

Corresponding Author

sven.julius.steinert@outlook.com

2 ABSTRACT

To raise information about the dominant location dependencies, a scenario was set up where an ISRU product is exported to an in-orbit depot and the total mass cost composition is analysed. In the selected scenario Oxygen is produced by an Ilmenite reduction plant and subsequently exported to the Lunar Gateway via a Oxygen-Hydrogen fueled launcher running in a round-trip, refueling Oxygen at the lunar outpost and Hydrogen at the Lunar Gateway. It showed that the variations in transport costs did have a neglectable influence on the total cost over an extended amount of time (+20 years) and therefore have a neglectable influence on the missions location selection in general.

Keywords: In situ resource utilization (ISRU), in-orbit fuel depot, lunar outpost, location selection, delta v map, Ilmenite reduction, Lunar Gateway, NRHO

1 INTRODUCTION

When a fully robotic ISRU production factory is feasible on the lunar surface, the location selection is not anymore bound to life support systems and the water resources they require. Therefore an optimization on the process factors can be applied to pick the most optimal location globally, instead being limited to polar regions only. For this event, this analysis is trying to identify the leading significance of the two sections of process factors, the ISRU efficiency (Section 2) and the Transport efficiency (Section 3), when an export aspect is considered. Hereby each section is inspected separately first before they are combined in a joined model (Section 4) to indentify the more relevant influence.

20 1.1 Scenario

In particular the ISRU production plant produces Oxygen as propellant component that is exported to an orbital propellant depot. The annual Oxygen production is 23.9 t (Chapter 2.1) that is transported via a round trip of a rocket launch system (Chapter 3.5) over [x] runs annually to the fuel-depot at target destination (Chapter 3.2). The mission duration is designed over a period of 10 years.

2 ISRU EFFICIENCY

When the optimal location is chosen by the highest ISRU efficiency, the whole production line has to be inspected for location dependent factors first. Such location dependent factors are for example: raw material concentration, solar irradiance, temperatures, flat surface conditions and further scenic requirements. Hereby, the production method is decisive about the sensitivity to location dependend factors. Where hydrogen reduction of ilmenite features a high dependency on the raw material concentration, molten regolith electrolysis for example is mostly invariant to it over the lunar surface. In this paper hydrogen reduction of ilmenite is chosen as the production method to be analysed, which we expect to have a rather strong location dependency. All results that are derived here are therefore only applicable to this single production method.

2.1 Model

To simplify model complexity, our model does include only the raw material concentration factor as argument, the Ilmenite weight ratio. While not covering all influences, this factor we are assuming the most significant for location dependency and serves as our approximation to the full model of hydrogen reduction of ilmenite. The goal here is not to give a precise value but to get in the right order of magnitude for a comparison later. The model cost is defined as the hardware mass that has to be moved to the lunar surface for ISRU operation which is to be minimized. In a previous work of (Guerrero-Gonzalez and Zabel, 2023) this hardware mass depending on Ilmenite concentration was determined for a combined production plant of Low Carbon Steel and Oxygen production. This production plant was sized for an annually output of 23.9 t Oxygen and 25 t Low Carbon Steel. The model consists out of a sum of required subsystems as defined in Equation 1 below.

$$\begin{aligned}
 y_0(x) &= 4036 \cdot x^{-1.064} - 9.59 && \text{Excavation} \\
 y_1(x) &= 17580 \cdot x^{-1.003} - 390.8 && \text{Handling} \\
 y_2(x) &= 19240 \cdot x^{-1.003} - 421.9 && \text{Beneficiation} \\
 y_3(x) &= 21780 \cdot x^{-1.198} + 120.3 && \text{O2 Extraction} \\
 y_4(x) &= 17910 \cdot x^{-1.265} + 1370 && \text{O2 Purification} \\
 y_5(x) &= 29650 \cdot x^{-0.7005} - 602.5 && \text{Metal Processing} \\
 y_6(x) &= 2541 \cdot x^{-0.7434} + 286.8 && \text{Gas Liquefaction \& Storage} \\
 y_7(x) &= 32440 \cdot x^{-0.8312} + 125.2 && \text{Thermal Control} \\
 y_8(x) &= 12000 \cdot x^{-0.9657} + 63.99 && \text{Power}
 \end{aligned}$$

45

$$m_{\text{hardware}}(x = w_{\text{ilmenite}}) = \sum_{i=0}^8 y_i(x) \quad (1)$$

Where in our scenario only the Oxygen production is relevant, the additional subsystems as Metal Processing scale in a similar way as the rest of the system so that the spread between low and high values of x is not distorted significantly (88.69% spread to the maximum value vs. 89.97% spread without Metal Processing, with $1 \leq x \leq 11$). Furthermore this combined production plant could still be a viable choice

50 out of the synergetic effects of shared infrastructure. This is why we are choosing this to be our reference
 51 production plant as a whole rather than attempting trimming subsystems. Therefore our model is expressed
 52 in Equation 1 as well.

53 2.2 Data Processing

54 To determine the cost for every location on the moon, a global lunar map of Ilmenite weight ratio is
 55 required. In a previous work by Hiroyuki (Sato et al., 2017) an almost global TiO₂ abundance map was
 56 created, where the values of weight percent for TiO₂ are used as equivalent for Ilmenite. The resulting
 57 map had a mask applied to leave only lunar mare regions and had a limited latitude coverage from 70° S to
 58 70° N. The limited coverage is caused by the sensor method to measure the reflectance of sunlight which
 59 is working less reliable with an increasingly steep sunlight angle towards the poles. The initial data was
 60 created by the Lunar Reconnaissance Orbiter Camera (LROC) Wide Angle Camera (WAC) which will be
 61 our starting point for the creation of our global Ilmenite map. First, the WAC data segments have been
 62 joined together resulting in a 27360 × 10640 resolution of 8-bit encoded values, plotted in Figure 1 below.

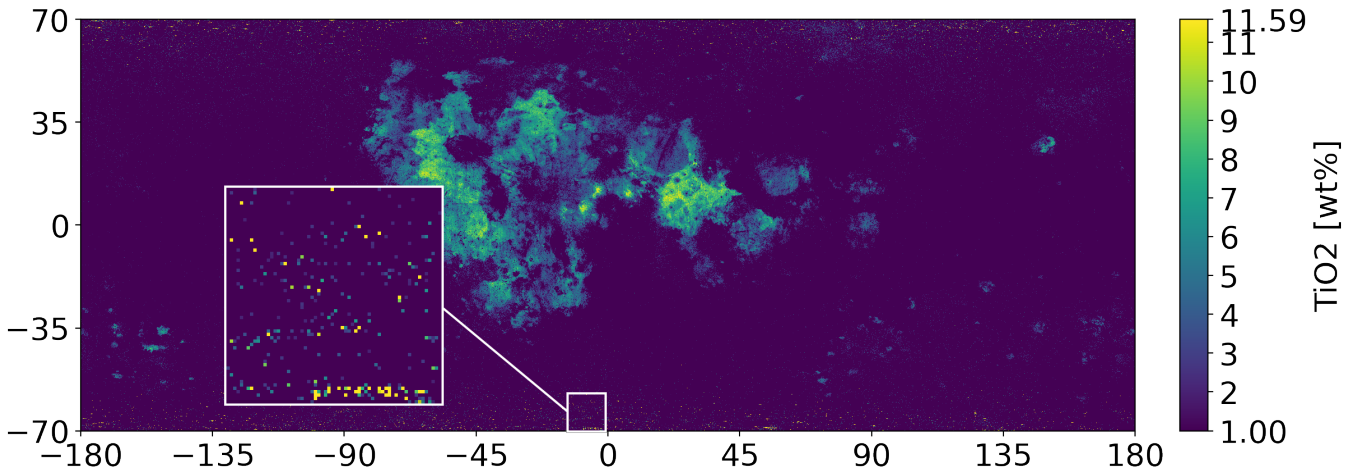


Figure 1. Combined original TiO₂ data of the WAC, (Sato et al., 2017)

63 2.2.1 Cleanup and Estimation

64 One problem are unusual high measurements towards the poles that are considered increasing noise
 65 which is scattered through the entire longitudinal axis. The second problem is the incomplete coverage of
 66 latitude and therefore the poles itself. To derive an estimation over the missing information at latitudinal
 67 coverage, the following strategy was applied. If Ilmenite abundance correlates with the classification of
 68 highlands/ mare and the pole regions geology is featuring highland characteristics then the expected value
 69 of the known highland region serves as an estimate of Ilmenite content at the poles.

70 As Figure 2 shows, the distribution characteristics of these two regions deviate considerably, whereby
 71 the average abundance also differs from 3,38 wt% in Mare to 1,1 wt% in Highland regions. Therefore the
 72 Ilmenite content correlation is given and the estimate over the missing latitudinal area of Highlands is set to
 73 1 wt% which also matches the WAC original assumption for values under the detection ratio. To additionally
 74 remove the increasing noise at further extreme latitudes, a mask is created out of mare boundaries from
 75 (Nelson et al., 2014) merged with a constant separation at ±56 deg latitude. The replacement values

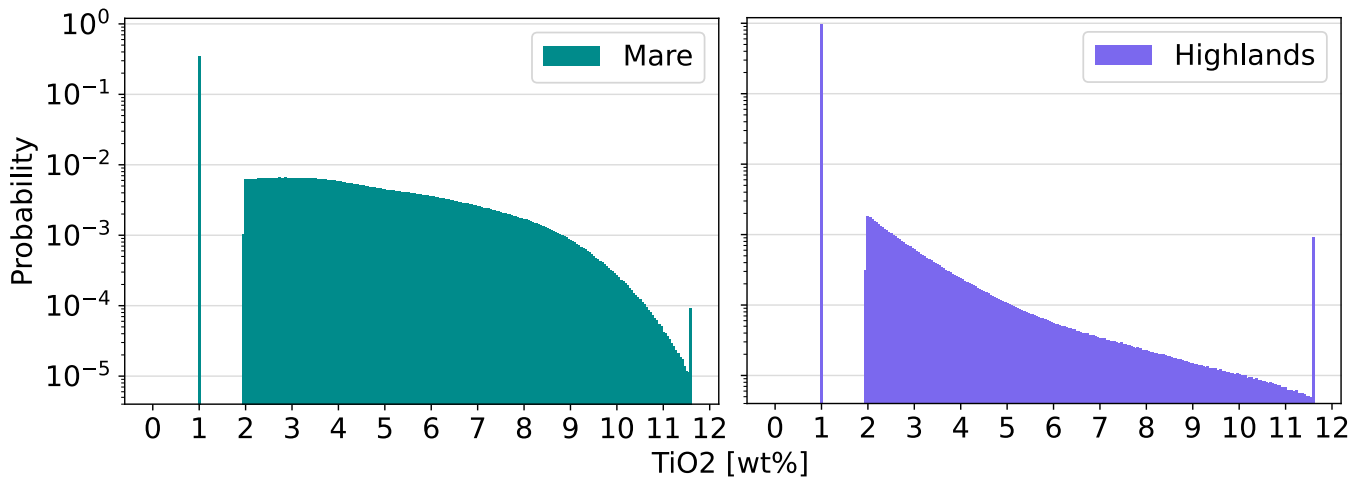


Figure 2. Distribution of Ilmenite content clustered into Highlands and Mare (equirectangular corrected) on combined WAC data with Mare boundaries from (Nelson et al., 2014)

76 for the mask are equally set to 1 wt%. With both estimates applied, a low noise global Ilmenite map is
77 accomplished which can be seen in Figure 3 below.

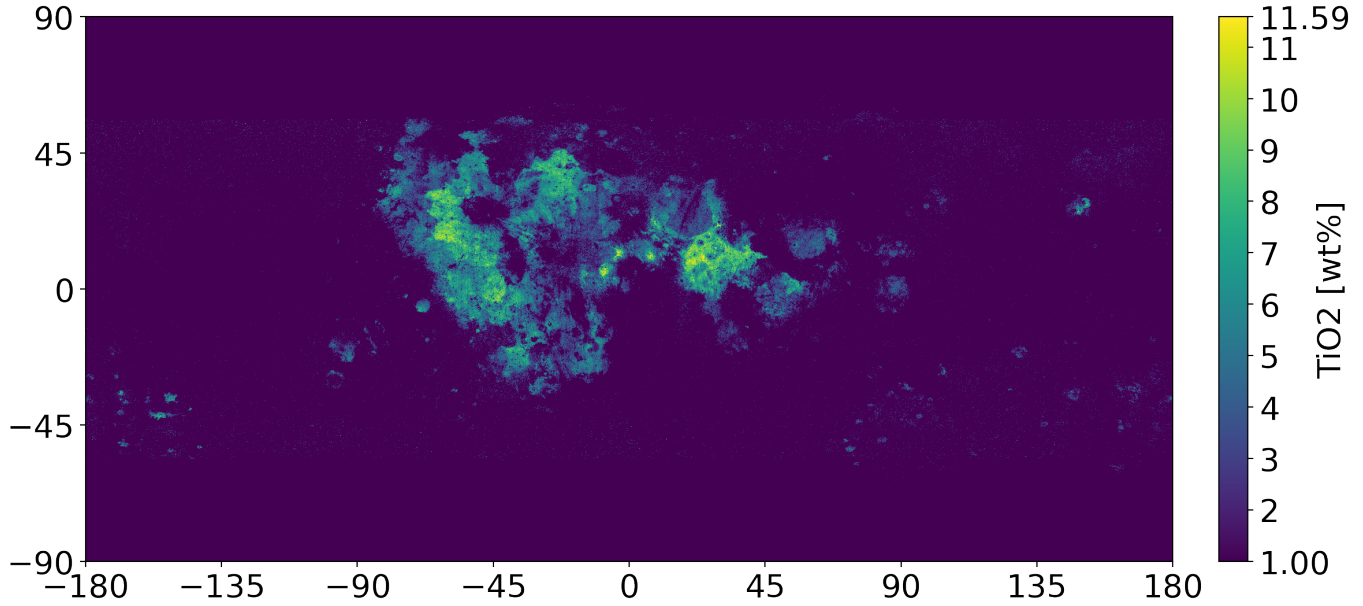


Figure 3. Global Ilmenite map based on WAC and estimates

78 2.2.2 Result

79 This global Ilmenite map from Figure 3 is now used as input to Equation 1, which results in the global
80 ISRU cost map displayed in Figure 4. The original resolution from the combined WAC data was kept
81 and only extended latitudinal, resulting in a size of 27360 × 13680 pixels, that corresponds to a geodetic
82 resolution of ≈ 400 m per pixel at the equator.

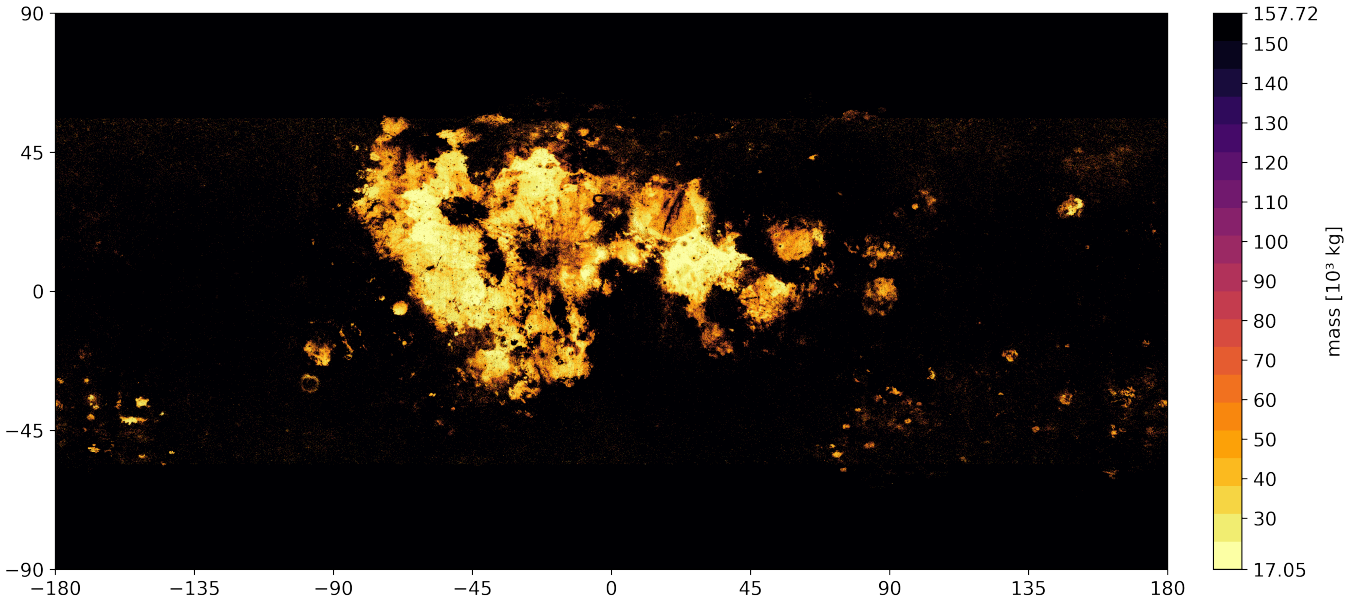


Figure 4. Global mass cost map for hardware by ISRU efficiency as base configuration

3 TRANSPORT EFFICIENCY

83 3.1 Mission Planning

84 The mission is designed to be carried out by a single stage launcher to loop between the lunar surface
 85 and the target orbit destination. The Oxygen fuel component and the Oxygen payload are refilled on lunar
 86 ground at the ISRU production plant. The Hydrogen fuel component on the other hand is refilled at the
 87 fuel depot where also the Oxygen payload is delivered. This results effectively in an exchange of delivered
 88 Oxygen to deducted Hydrogen from the station. A multi staged launcher or a shuttle exchange system was
 89 neglected for this analysis but would hold the potential to further increase transport efficiency.

90 3.2 Fuel Depot Location

91 As in-orbit depot and their requirement of a widely accessible logistic hub from multiple locations,
 92 Liberation points or Halo orbits are especially suited. In the case of the Moon, the currently planned Lunar
 93 Gateway on its Near-rectilinear halo orbit (NRHO) fits prodigiously these requirements. Which is why the
 94 Lunar Gateway is chosen to be analysed in this scenario as the export destination.

95 3.3 Target Orbit

96 For the selected fuel depot location at the Lunar Gateway, the target orbit is a specific NRHO that is in a
 97 9:2 Lunar Synodic Resonance with an average perilune of $h_{peri} = 3557 \text{ km}$ and an average orbital period
 98 of $T = 6.562 \text{ days}$ (Lee, 2019). It is worth mentioning that this orbit has a varying polar crossing as well
 99 as other time dependent changes in its trajectory which are often simplified to more static conditions for
 100 analysis (Whitley et al., 2018).

101 3.4 Δv Estimation

102 First of all, regardless of the mission or the trajectory, planetary conditions such as ground elevation and
 103 ground speed are influencing the required Δv . These influences are now briefly assessed for the moon to
 104 determine their relevance.

105 3.4.1 Planetary influences

106 The initial radial distance to the planets center of mass $r(\phi, \lambda)$ influences the Δv demand directly as
 107 shown for an ascent into a circular orbit at r_{orbit} in equation 2 below.

$$\Delta v_{ideal}(\phi, \lambda) = \sqrt{v_{orbit}^2 + v_{ascent}^2} = \sqrt{\left(\frac{\mu}{r_{orbit}}\right) + \left(2 \cdot g_0 \cdot \left[r(\phi, \lambda) - \frac{r(\phi, \lambda)^2}{r_{orbit}}\right]\right)} \quad (2)$$

108 Global ground elevation data is now used in the form of a displacement map, which originates on LOLA
 109 measurements. The elevation ranges from -9.115 km to 10.757 km with regard to the reference radius r_{ref}
 110 of 1737.4 km and therefore defines $r(\phi, \lambda)$ globally. The displacement map is shown in Figure 5 below.

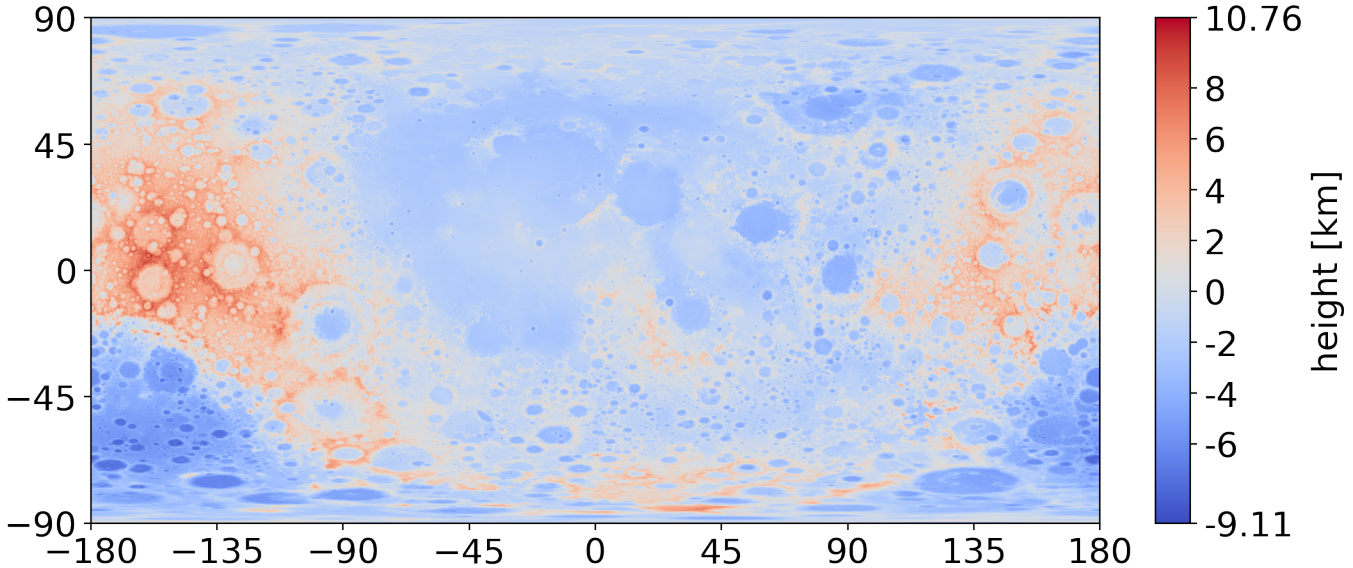


Figure 5. Lunar displacement map to reference radius ($r_{ref} = 1737.4\text{km}$). Data from NASA CGI Kit (Wright and Petro, 2019) based on (David E. Smith, 2015)

Evaluating the extreme values with Equation 2 on a 100 km LLO ($r_{orbit} = 1837.4\text{km}$) yields:

$$\begin{aligned}\Delta v_{min} &= \Delta v_{ideal}(\max \{r(\phi, \lambda)\}) = 1725.187 \frac{\text{m}}{\text{s}} \\ \Delta v_{max} &= \Delta v_{ideal}(\min \{r(\phi, \lambda)\}) = 1725.204 \frac{\text{m}}{\text{s}}\end{aligned}$$

111 The influence on Δv from ground elevation is therefore at the order of 0.001 % which is extremely low.
 112 The second planetary influence, the initial ground speed v_0 is either an additional Δv demand or a Δv
 113 reduction, depending on the shared velocity components to the launch direction. Together with the sidereal
 114 rotation period and the assumption of a spherical lunar surface of r_{ref} , the ground speed can be given as a
 115 function of Latitude ϕ as displayed in Equation 3.

$$v_0(\phi) = \frac{2\pi}{27.322 \text{ days}} \cdot \cos(\phi) \cdot r_{\text{ref}} \quad (3)$$

116 Evaluating the extreme points of polar and equatorial locations on Equation 3 yields:

$$\begin{aligned}\Delta v_{\min} &= \Delta v_0(\phi = 90 \text{ deg}) = 0.000 \frac{\text{m}}{\text{s}} \\ \Delta v_{\max} &= \Delta v_0(\phi = 0 \text{ deg}) = 4.624 \frac{\text{m}}{\text{s}}\end{aligned}$$

117 Comparing this range $\Delta v_{\max} - \Delta v_{\min}$ to the ascent of a circular 100 km LLO to reference radius
 118 $\Delta v_{\text{ideal}}(r_{\text{ref}}) = 1725.196 \frac{\text{m}}{\text{s}}$ gives the Δv influence of the ground speed to be at the order of 0.27 % which
 119 is significantly more than the elevation influences but still considerably low.

120 3.4.2 Transfer options

121 Explicit Transfers from any lunar geodetic point to NRHOs and vice versa are a high-fidelity problem
 122 which is usually solved non-analytically. Additionally there are multiple transfer strategies that can be
 123 deployed for different optimisation goals. Between optimisation of required Δv and transfer time, 2 transfer
 124 options are being analysed for our chosen scenario.

125 First, a long duration transfer that features a very low required Δv of only $664.9 \frac{\text{m}}{\text{s}}$ to a 100 km LLO,
 126 which is very close to the theoretical limit of $654.8 \frac{\text{m}}{\text{s}}$ as minimum energy change (Whitley et al., 2018).
 127 Also, it features an almost complete independency to surface location, which is reached by something
 128 similar as a Three-Impulse transfer, where the lunar sphere of influence is left to circle once around earth
 129 before inserting again. This allows any inclination restrictions to vanish, but at a cost of a 100.1 day long
 130 transfer time. This first, long transfer option is displayed in Figure 6 below.

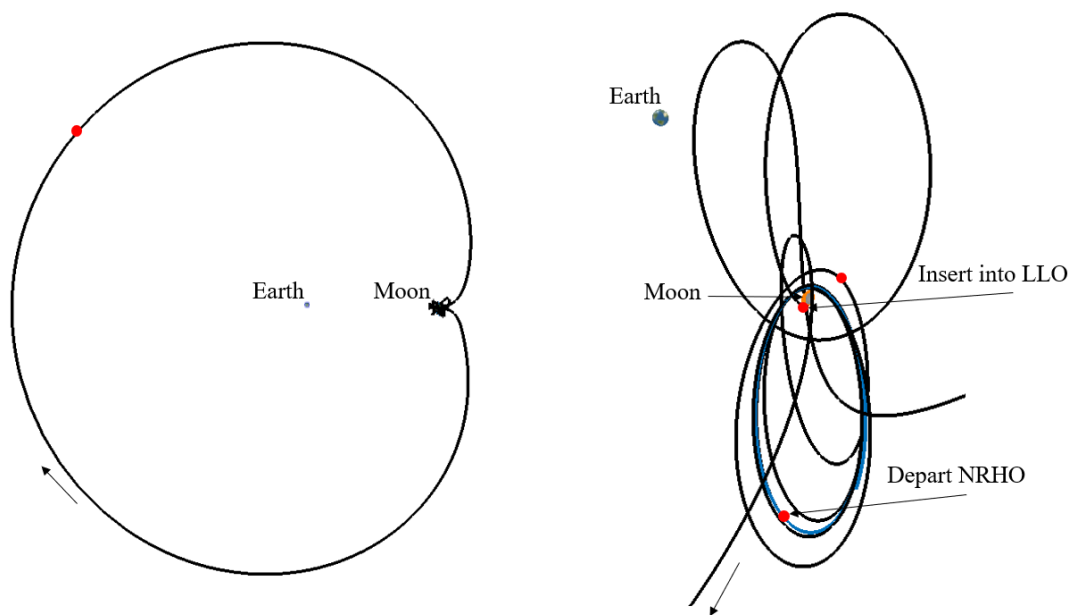


Figure 6. “100.1 day transfer from the 9:2 NRHO to 100 km altitude LLO requiring 664.9 m/s with maneuvers marked in red” – (Whitley et al., 2018)

If this transfer option is chosen, the influence of transfer efficiency is at an order of the planetary influences mentioned in Section 3.4.1 and therefore marginal to the ISRU dependencies derived in Chapter 2. In this case transfer dependencies can be neglected and the location selection can be simplified to only ISRU efficiency.

Often however a 100 day transfer time is simply to long for certain applications, as it for example induces general system lag time and therefore poor dynamics in propellant delivery adjustments in the case of our mission. For this reason, a second transfer option is analysed which is a direct transfer trajectory between the NRHO and the surface which features the shortest transfer time of only hours but at the cost of a higher Δv .

3.4.3 Data processing

In a previous work, a set of possible trajectories was identified through a spherical search [cite]. The resulting map of samples for the 9:2 NRHO was taken as starting point for a global Δv map. From there, square tiles are created wherein the Δv is assumed to be constant and the value for the tile was set by the minimum Δv of the possible trajectories within the tile. This was done with various tile sizes between xx and xx deg to find a suitable estimate, displayed in Figure xx below.

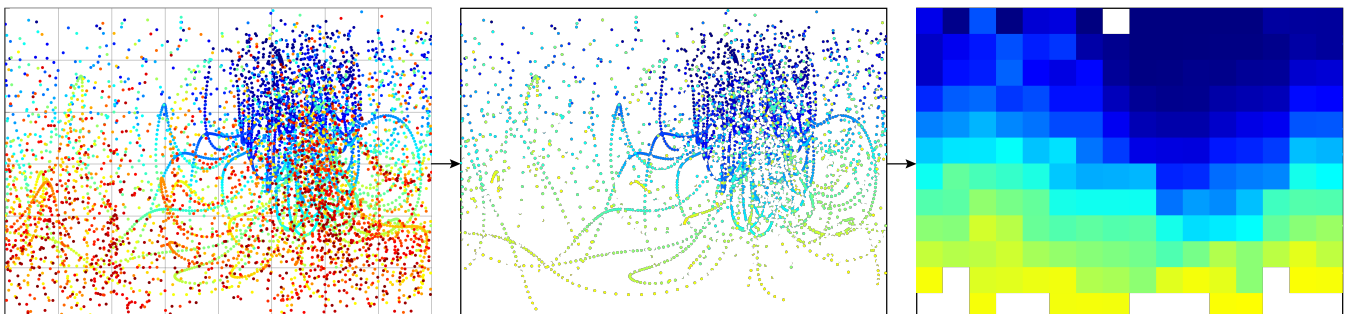


Figure 7. Processing of results from [cite] to cutting of data to tiling of minimum

The resulting tiled Δv map was filled by by interpolations resulting in our final estimation for Δv requirements from any surface point into the 9:2 NRHO displayed in Figure xx below.

3.4.4 Result

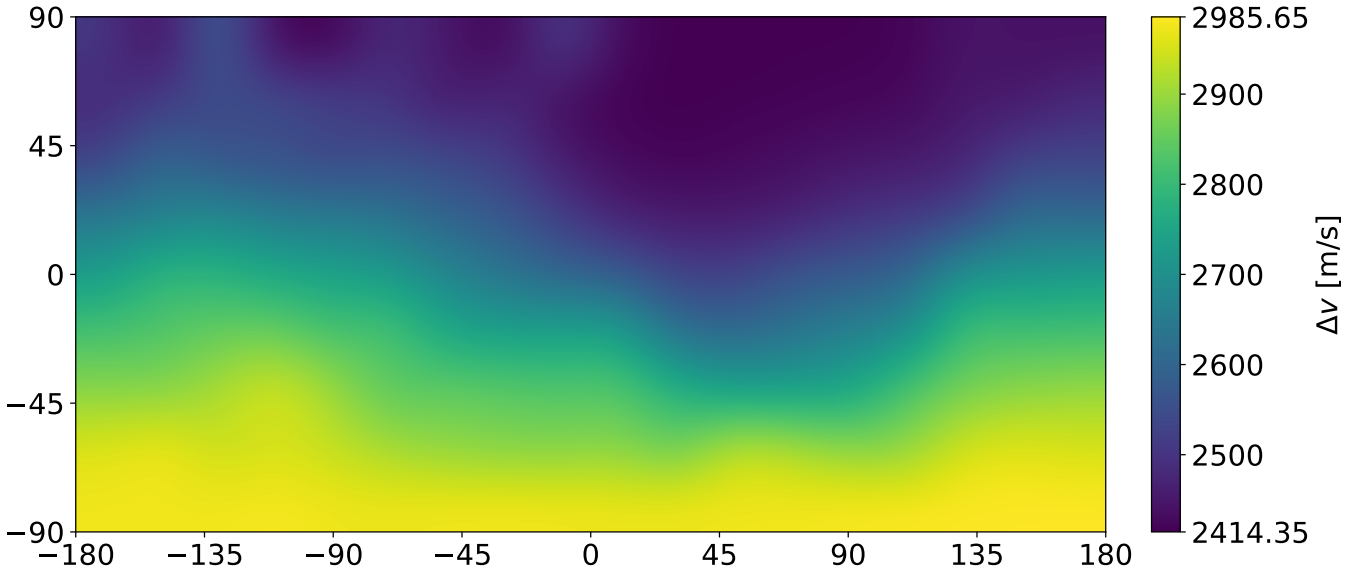


Figure 8. Required Δv for direct decent from Southern 9:2 NRHO to Lunar Surface (bicubic interpolated)

149 3.5 Transport Carrier

150 3.5.1 Reference Launcher

151 To derive associated transport mass costs, the previously computed delta v has to be applied on a specific
 152 launcher. The Argonaut, formerly known as the European Large Logistics Lander (EL3), is chosen as a
 153 starting point for this mission. The initial configuration is based on the time of writing published information
 154 of 8500 kg wet mass, 1600 kg drymass and 1500 kg payload. [cite] Additionally a Hydrogen, Oxygen
 155 propulsion system with an o/f ratio of 6 and 400 s of specific impulse are assumed. When this original
 156 configuration is applied on our mission (Table XX), the fuel runs out before completing the round-trip.
 157 This can also be anticipated from the maximum delta v of the launcher $\Delta v_{\text{Argonaut}} = I_{sp} \cdot g_0 \cdot \ln(\frac{m_0}{m_f}) =$
 158 $3958 \frac{m}{s} < \Delta v_{\text{total}} \approx 2 \cdot \Delta v_{\text{NRHO,min}}$.

159 3.5.2 Upscaling

160 From there on an up-scaling is performed, where the drymass is kept constant at 1600 kg but fuel is added
 161 until the mission can be completed. The minimal viable system features an empty H₂ tank at arrival at the
 162 Gateway and an empty O₂ tank at the lunar surface. The Iteration scheme of the upscaling is visualized in
 163 Figure 9 which can now converge a minimal viable launcher for any given payload.

164 In the mission table 1 below is shown the converged upscale for the standard EL3 payload of 1500 kg.

	ΔV	$\Delta H2$	$\Delta O2$	mass	H2	O2	payload
Lunar Surface			+6248	10063	715	6248	+1500
Maneuvers	2695.38	-714	-4287	5062	1	1961	
Gateway exchange		+1042		4604	1043	1961	-1500
Maneuvers	2695.38	-327	-1961	3816	716	0	
==== SUCCESS ===	=====	=====	=====	=====	=====	=====	=====

Table 1. Mission table with up-scaled configuration at 1500 kg payload

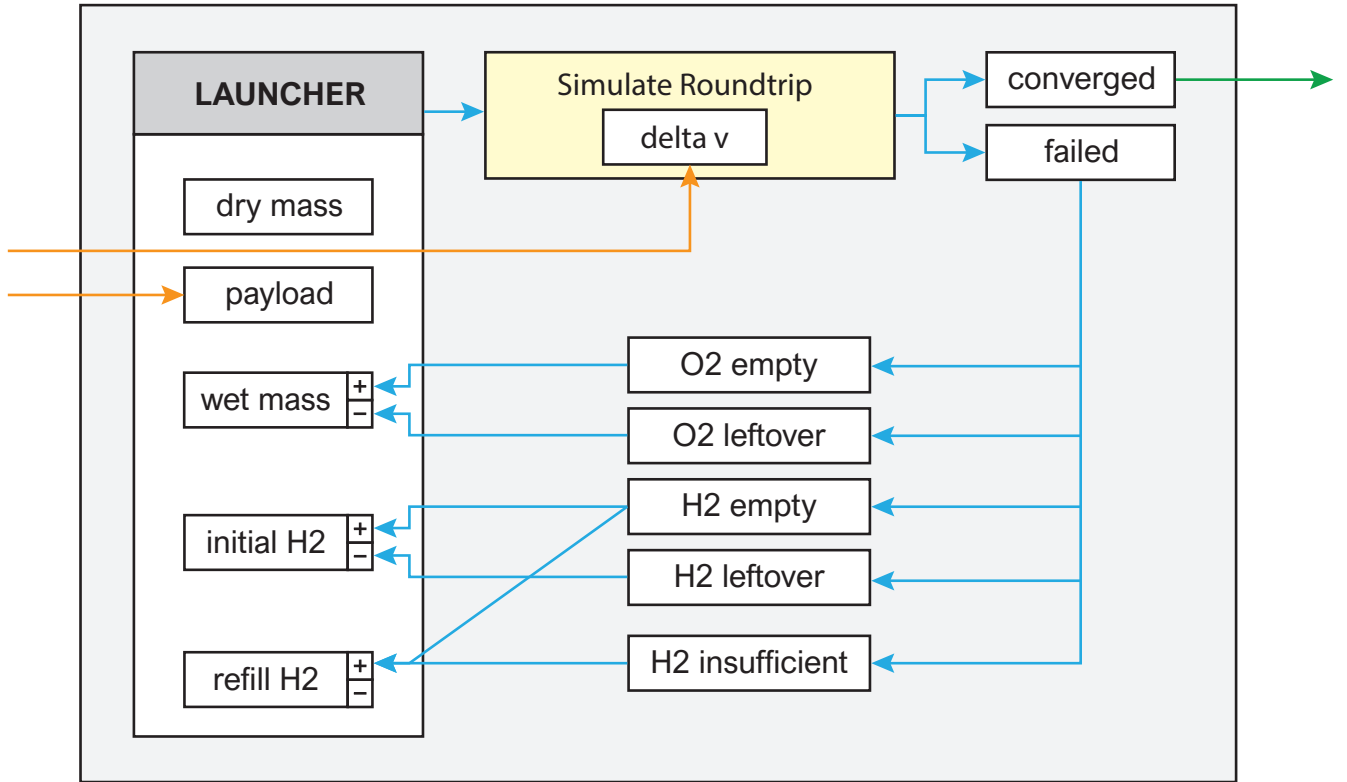


Figure 9. Launcher iteration to converge a roundtrip for a given payload and Δv

165 exchange ratio of Oxygen delivered to Hydrogen taken at the Gateway With the ability to converge a
 166 launcher in this manner, the payload is a degree of freedom where over a sweep was performed. In Figure
 167 ?? the increasing exchange ratio is visible.

168 Since this method of up-scaling is effectively increasing the mass ratio of the launcher, this assumption
 169 becomes increasingly unrealistic. In order to

170 3.5.3 Fuel Costs

171 3.5.4 Result

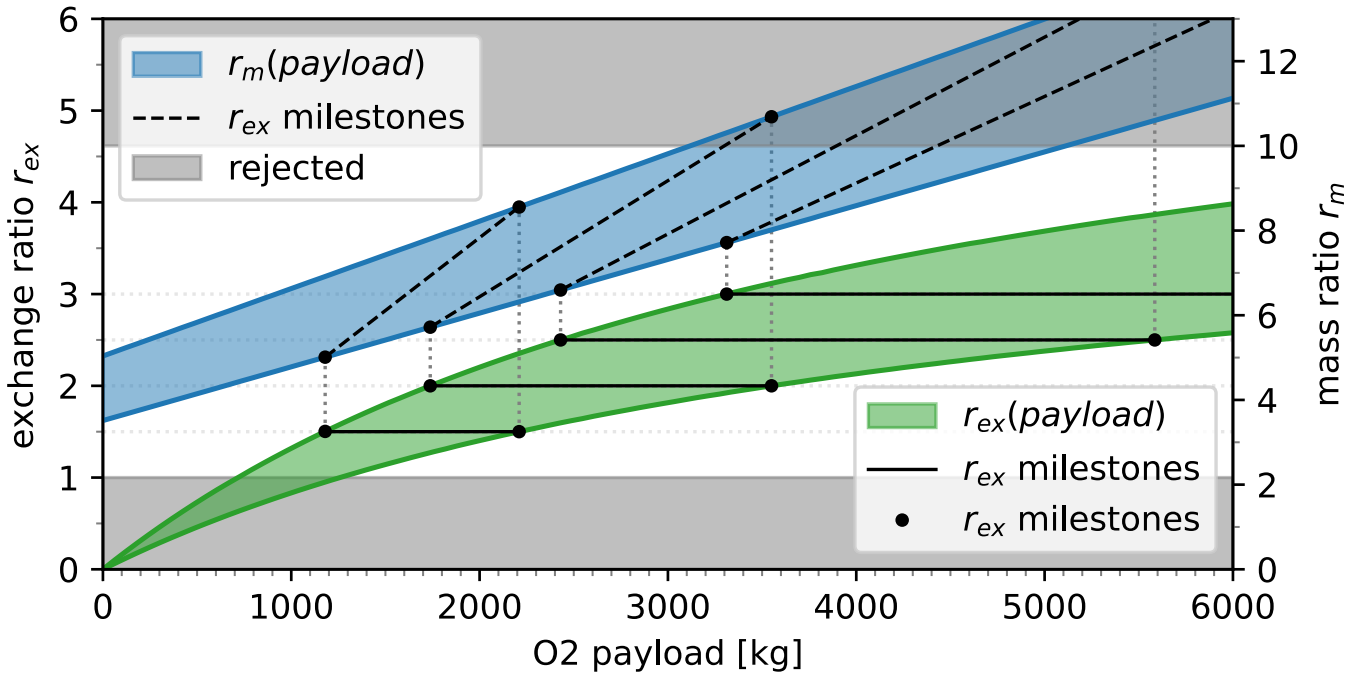


Figure 10. Exchange ratio r_{ex} and mass ratio r_m depending on payload size of the launcher in Δv range

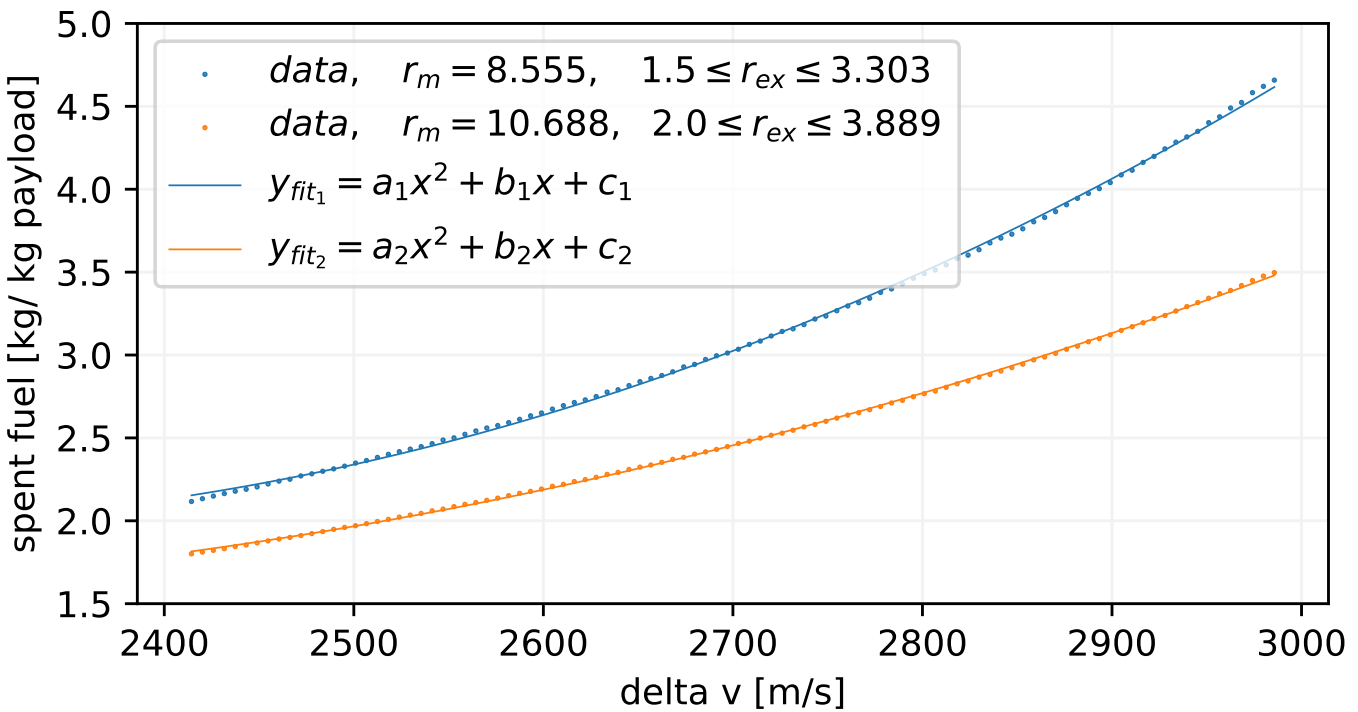


Figure 11. relationship between required delta v and spend fuel per kg payload

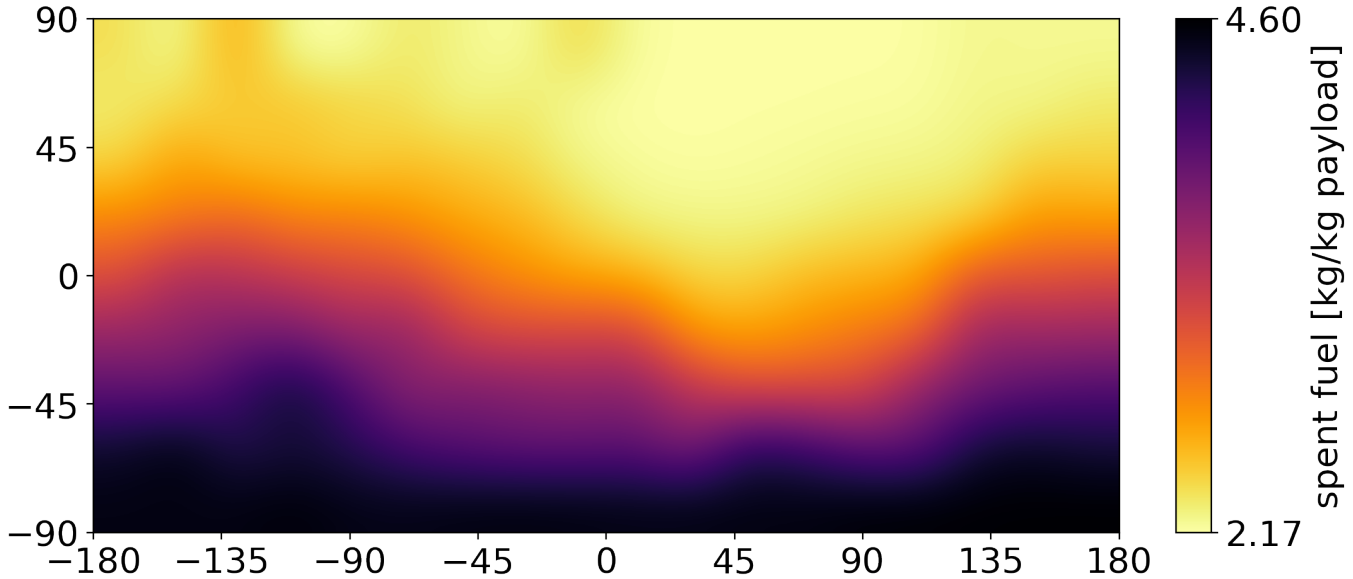


Figure 12. Location dependent spend fuel to the 9:2 NRHO per kg payload with $r_{\text{ex}} = 1.5$

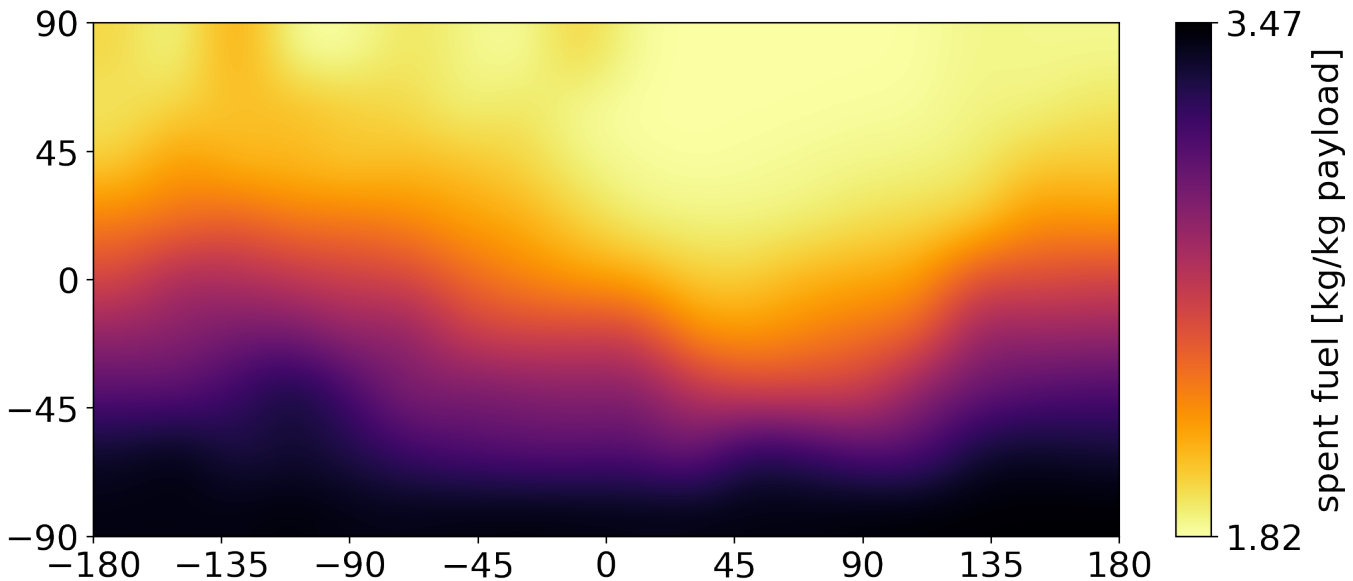


Figure 13. Location dependent spend fuel to the 9:2 NRHO per kg payload with $r_{\text{ex}} = 2.5$

4 JOINED MODEL - RELEVANCE COMPARISON

173 4.1 Total Cost Modelling

174 When both influences from A and B are combined, the comparable mass costs have to be drawn from
 175 the mission scenario. Rather than assuming all expended fuel as transport cost, a separation of the fuel
 176 components is done, due to Oxygen is not being planned to be shipped from Earth but rather fully be
 177 supplied by the ISRU facility.

178 4.1.1 Fix Costs

179 In order to meet the additional demand of Oxygen per year m_{+Ox} , the ISRU facility is scaled up
 180 linearly by its ISRU costs per kg Oxygen k_{ISRU} for each location and its corresponding fuel requirements.
 181 Therefore the fix costs, which represent the mass for the construction of the ISRU facility are:

$$K_{\text{Fix}}(\phi, \lambda) = K_{\text{base}}(\phi, \lambda) + k_{\text{ISRU}}(\phi, \lambda) \cdot m_{+Ox}(\phi, \lambda, r_{\text{ex}}) \quad (4)$$

182 4.1.2 Dynamic Costs

183 The expended Hydrogen, which is derived by the oxidiser-fuel-ratio r_{of} , is considered fully as mass cost
 184 since it is taken from the Lunar Gateway Depot. Hereby the cost level of Lunar Gateway and lunar surface
 185 are simplified as equal to be comparable, which rather overestimates the Hydrogen's cost in comparison to
 186 costs on the lunar surface when supplied from Earth. Depending on the exchange ratio $r_{\text{ex}} \in \{1.5, 2.5\}$
 187 that leads to the spend fuel per kg payload k_{Flight} , the dynamic mass costs per year t are:

$$K_{\text{Dynamic}}(\phi, \lambda, t) = t \cdot k_{\text{Flight}}(\phi, \lambda, r_{\text{ex}}) \cdot \frac{1}{r_{\text{of}} + 1} \quad (5)$$

188 4.1.3 Total Costs

189 Combining both fix costs and dynamic costs, the final total costs in location and time dependency are

$$K_{\text{Total}}(\phi, \lambda, t) = K_{\text{Fix}}(\phi, \lambda) + K_{\text{Dynamic}}(\phi, \lambda, t) \quad (6)$$

190 4.2 Result

191 4.2.1 Mission Evaluation

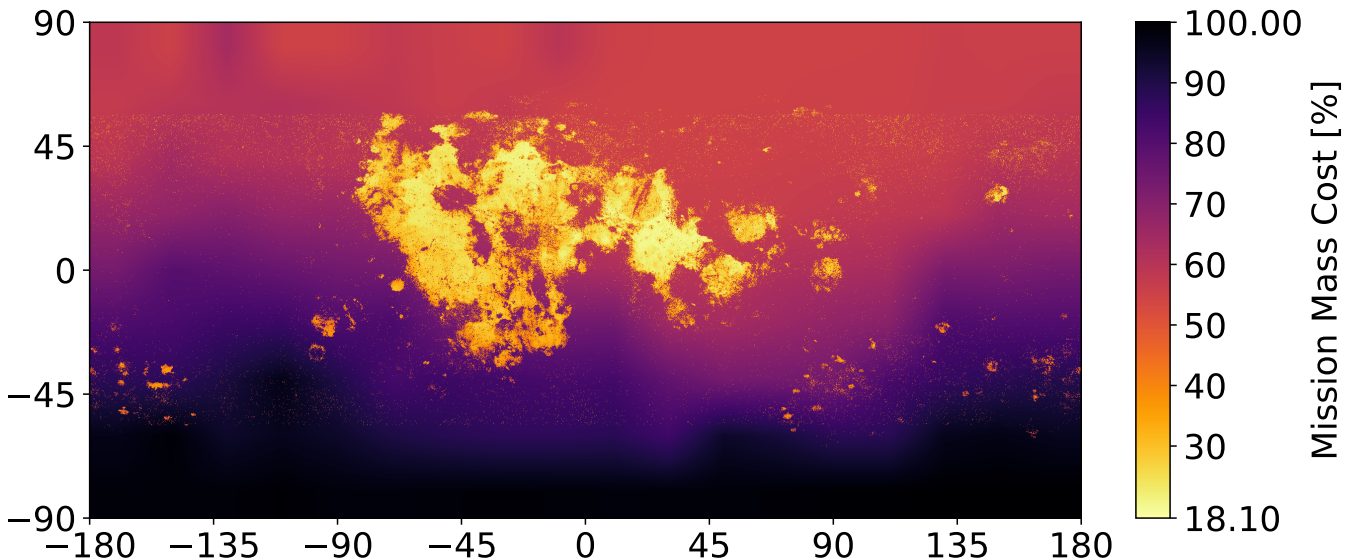


Figure 14. Total Cost Map in percentage after a mission duration on 20 years $r_{\text{ex}} = 1.5$

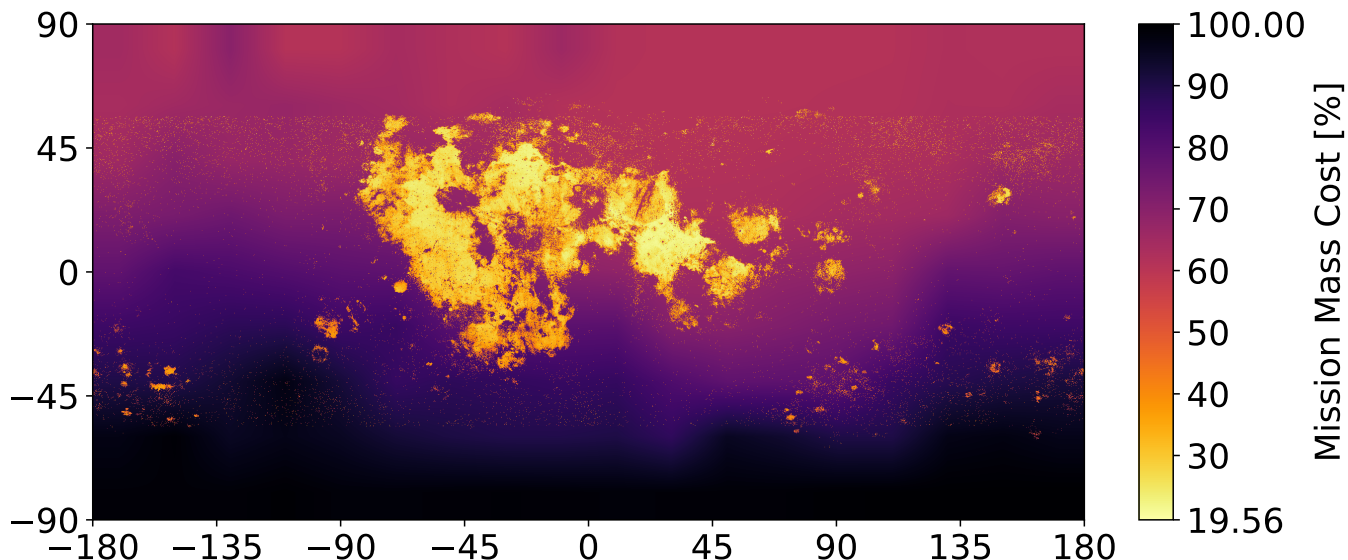


Figure 15. Total Cost Map in percentage after a mission duration on 20 years $r_{\text{ex}} = 2.5$

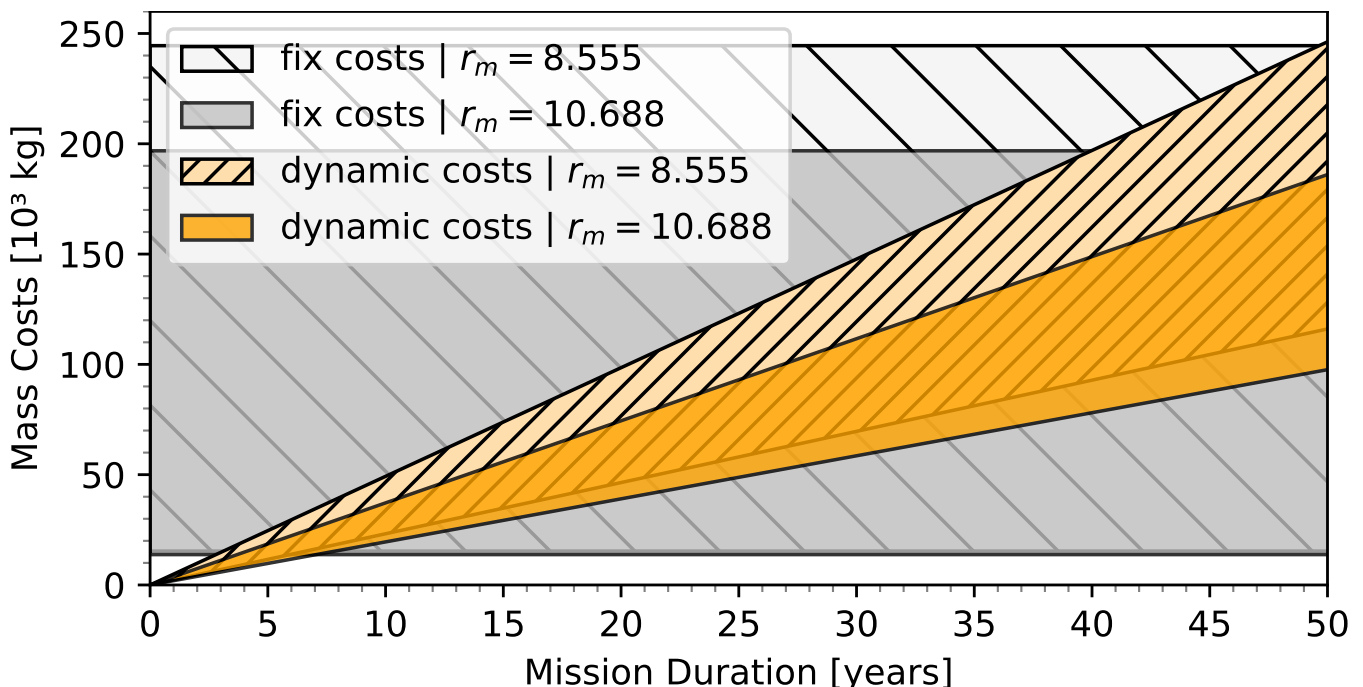


Figure 16. Cost components form both $r_{\text{ex}} = 2.5$ and $r_{\text{ex}} = 2.5$

192 4.2.2 Break Even

193 4.2.3 General Result

5 OUTLOOK

CONFLICT OF INTEREST STATEMENT

194 The authors declare that the research was conducted in the absence of any commercial or financial
195 relationships that could be construed as a potential conflict of interest.

AUTHOR CONTRIBUTIONS

196 The Author Contributions section is mandatory for all articles, including articles by sole authors. If an
197 appropriate statement is not provided on submission, a standard one will be inserted during the production
198 process. The Author Contributions statement must describe the contributions of individual authors referred
199 to by their initials and, in doing so, all authors agree to be accountable for the content of the work. Please
200 see here for full authorship criteria.

FUNDING

201 Details of all funding sources should be provided, including grant numbers if applicable. Please ensure to
202 add all necessary funding information, as after publication this is no longer possible.

ACKNOWLEDGMENTS

203 This is a short text to acknowledge the contributions of specific colleagues, institutions, or agencies that
204 aided the efforts of the authors.

SUPPLEMENTAL DATA

205 Supplementary Material should be uploaded separately on submission, if there are Supplementary Figures,
206 please include the caption in the same file as the figure. LaTeX Supplementary Material templates can be
207 found in the Frontiers LaTeX folder.

DATA AVAILABILITY STATEMENT

208 This work is providing open source on the complete processing steps in the corresponding Python Notebooks
209 along with all resources in full resolution at the papers [Git-Repository](#).

210 The datasets [GENERATED/ANALYZED] for this study can be found in the [NAME OF REPOSITORY]
211 [LINK].

REFERENCES

- 212 [Dataset] David E. Smith (2015). 2009 lunar orbiter laser altimeter radiometry data set, lro-l-lola-3-radrr-
213 v1.0. doi:10.17189/1520639
- 214 Guerrero-Gonzalez, F. J. and Zabel, P. (2023). System analysis of an ISRU production plant: Extraction of
215 metals and oxygen from lunar regolith. *Acta Astronautica* 203, 187–201. doi:10.1016/j.actaastro.2022.
216 11.050
- 217 Lee, D. E. (2019). National aeronautics and space administration (nasa) white paper: Gateway destination
218 orbit model: A continuous 15 year nrho reference trajectory
- 219 Nelson, D. M., Koeber, S. D., Daud, K., Robinson, M. S., Watters, T. R., Banks, M. E., et al. (2014).
220 Mapping lunar maria extents and lobate scarps using lroc image products. *Lunar Planet. Sci.* 45, 2861
- 221 Sato, H., Robinson, M. S., Lawrence, S. J., Denevi, B. W., Hapke, B., Jolliff, B. L., et al. (2017). Lunar
222 mare tio 2 abundances estimated from uv/vis reflectance. *Icarus* 296, 216–238. doi:10.1016/j.icarus.
223 2017.06.013
- 224 Whitley, R., Davis, D., Burke, L., McCarthy, B., Power, R., McGuire, M., et al. (2018). Earth-moon near
rectilinear halo and butterfly orbits for lunar surface exploration

226 [Dataset] Wright, E. and Petro, N. (2019). SVS: CGI Moon Kit — svs.gsfc.nasa.gov. [https://svs.
227 gsfc.nasa.gov/4720](https://svs.gsfc.nasa.gov/4720). [Accessed 29-07-2023]

FIGURE CAPTIONS